

Berry phase and ground-state symmetry in $H \otimes h$ dynamical Jahn-Teller systems

Nicola Manini

European Synchrotron Radiation Facility, Boîte Postale 220, F-38043 Grenoble Cédex, France

Paolo De Los Rios

Institut de Physique Théorique, Université de Fribourg, 1700-CH Fribourg, Switzerland

(Received 3 March 2000)

Due to the ubiquitous presence of a Berry phase, in most cases of dynamical Jahn-Teller systems the symmetry of the vibronic ground state is the same as that of the original degenerate electronic state. As a single exception, the linear $H \otimes h$ icosahedral model is determined by an additional free parameter, which can be continuously tuned to eliminate the Berry phase from the low-energy closed paths: accordingly, the ground state changes to a totally symmetric nondegenerate state. The detailed values of the parameters not being known, the issue of the actual ground-state symmetry of C_{60}^+ is open.

The traditional field of degenerate electron-lattice interactions (Jahn-Teller effect) in molecules and impurity centers in solids^{1,2} has drawn interest in recent years, excited by the discovery of new systems calling for a revision of a number of commonly accepted beliefs. Several molecular systems including C_{60} ions, higher fullerenes, and Si clusters, derive their behavior from the large (up to fivefold) degeneracy of electronic and vibrational states due to the rich structure of the icosahedral symmetry group.³ Jahn-Teller (JT) systems have therefore been considered theoretically,^{2,4,5} disclosing intriguing features,⁵⁻⁹ often related to a Berry phase¹⁰ in the electron-phonon coupled dynamics.

As it is well known, the molecular symmetry, reduced by the JT distortion with the splitting of the electronic-state degeneracy, is restored in the dynamical Jahn-Teller (DJT) effect, where tunneling among equivalent distortions is considered. The vibronic states are therefore labeled as representations of the original point group of the undistorted system. In particular, for continuity, the weak-coupling ground state (GS) retains the same degenerate representation as that labeling the electronic level prior to coupling. *A priori*, there is no particular reason for this to continue at larger couplings. However, it appears empirically² that in all linear DJT systems studied before the late nineties, the GS symmetry remains the same at all couplings. The explanation of this observation was a great outcome of the Berry-phase¹⁰ scenario: the phase entanglement in the electron-phonon Born-Oppenheimer (BO) dynamics,^{5,11-13} originating at electronically degenerate high-symmetry points, seemed a universal feature of the DJT systems.

In this context, it came as a surprise the discovery of the first linear JT system showing a *nondegenerate* GS in the strong-coupling limit.^{8,9} In particular, Ref. 8 studied a spherical model $D \otimes d$ ($L=2$ electrons interacting with $L=2$ vibrations). This system turns out to be a special case of the $H \otimes h$ icosahedral model: a fivefold degenerate H electronic state interacting linearly with a distortion mode of the same symmetry h .^{8,14} In that special case, it was shown that, for increasing coupling, a nondegenerate A excited state in the vibronic spectrum moves down, to cross the H GS at some finite value of the coupling parameter, thus becoming the GS

at strong coupling.⁸ This phenomenon is a manifestation of a vanishing Berry phase in the entangled JT dynamics.^{8,15}

The examples examined in the literature^{8,9} are very specific, and hardly related to a realistic case such as, for example, C_{60}^+ . In this paper, we study the linear $H \otimes h$ model in its generality. We analyze in detail the connection between the symmetry/degeneracy of the vibronic GS and the presence/absence of a Berry phase in the coupled dynamics. This model owns its peculiarities to the *nonsimple reducibility* of the icosahedral symmetry group. In particular, the H representation appears twice in the symmetric part of the Kronecker product of the H representation with itself:

$$\{H \otimes H\}^{(s)} = a \oplus g \oplus h^{[1]} \oplus h^{[2]}. \quad (1)$$

There are, therefore, two independent sets of Clebsch-Gordan (CG) coefficients,

$$C_{\mu,\nu}^{m[r]} \equiv \langle H, \mu; H, \nu | h, m \rangle^{[r]} \quad (2)$$

for the coupling of an H electronic state with an h vibrational mode, identified by a multiplicity index $r=1,2$.¹⁶ Of course, since the two h states are totally equivalent and indistinguishable, symmetrywise, the choice of these orthogonal sets of coefficients has some degree of arbitrariness: the free parameter α in the combination

$$C_{\mu,\nu}^m(\alpha) \equiv \cos \alpha C_{\mu,\nu}^{m[1]} + \sin \alpha C_{\mu,\nu}^{m[2]} \quad (3)$$

accounts for it. The coefficient $C_{\mu,\nu}^m(\alpha)$ coincides with the $r=1$ and $r=2$ values¹⁷ for $\alpha=0$ and $\alpha=\pi/2$, respectively. Also, for $\alpha = -\arctan(3/\sqrt{5}) \equiv -\alpha_s$, it becomes equivalent to the spherical CG coefficient.

The basic Hamiltonian for the $H \otimes h$ model can be written

$$H = H_{\text{harm}}(\hbar \omega) + H_{e-v}(g \hbar \omega, \alpha), \quad (4)$$

with

$$H_{\text{harm}}(\hbar \omega) = \frac{1}{2} \hbar \omega \sum_m (p_m^2 + q_m^2), \quad (5)$$

$$H_{e-v}(g\hbar\omega, \alpha) = \frac{g\hbar\omega}{2} \sum_{m\mu\nu} q_m c_{\mu}^{\dagger} c_{-\nu} C_{\mu,\nu}^m(\alpha), \quad (6)$$

where q_m is the distortion coordinate (with conjugate momentum p_m) and c_m^{\dagger} is the electronic operator in standard second-quantized notation.

The α dependence of the CG coefficients indicates that the group does not determine completely the form of the JT coupling as, for example, in cubic symmetry. The specific value of α must be established case by case by detailed analysis of the phonon mode and its coupling with that specific electronic state. Indeed, each h mode of, say, C_{60}^{+} ions, is characterized not only by its own frequency ω_i and scalar coupling g_i , but also by its particular angle of mixing α_i . Earlier works on $H \otimes h$ DJT studied in detail the cases $\alpha = \pi - \alpha_s$ (Ref. 8) and $\alpha = \pi/2$ (Ref. 9).

For intermediate to strong coupling, the interesting non-perturbative regime, the customary framework is the BO separation of vibrational and electronic motion: when the splitting among the five potential sheets (proportional to g^2) is large, the electronic state can be safely assumed to follow adiabatically the lowest BO potential sheet, while virtual inter-sheet electronic excitations may be treated as a small correction. The BO dynamics is determined by the lowest eigenvalue of the interaction matrix $\Xi = \sum q_m V^{(m)}$ in the electronic space. Ξ is obtained from Eq. (6) by the same technique described in Ref. 15, and it is a simple generalization of that obtained for $D \otimes d$: here, for brevity, we report only the expression of the diagonal matrix elements of the $V^{(0)}$ matrix, corresponding to the coupling to a pure q_0 distortion:

$$\begin{bmatrix} C_{0,2}^2(\alpha) \\ -C_{0,1}^1(\alpha) \\ C_{0,0}^0(\alpha) \\ -C_{0,1}^1(\alpha) \\ C_{0,2}^2(\alpha) \end{bmatrix} = \cos \alpha \begin{bmatrix} 1 \\ 2/\sqrt{5} \\ 1 \\ 2/\sqrt{5} \\ 1 \end{bmatrix} + \sin \alpha \begin{bmatrix} -1/2 \\ 1/2 \\ 0 \\ 1/2 \\ -1/2 \end{bmatrix}. \quad (7)$$

This form makes it clear that a shift $\alpha \rightarrow \alpha + \pi$ introduces a sign change in the coupling matrix, and it can be compensated by a reflection $\vec{q} \rightarrow -\vec{q}$. We will restrict ourselves therefore, without loss of generality, to the interval $0 \leq \alpha \leq \pi$.

The electronic eigenvalue $(-2/\sqrt{5})\cos \alpha$ is the lowest for $\alpha < \alpha_s$ and $\alpha > \pi - \alpha_s$ (region *a*): in this range the BO potential presents six absolute minima, one of which is lying along the \hat{q}_0 pentagonal axis, with energy lowering $E_{\text{clas}} = -g^2 \cos^2 \alpha \hbar \omega / 10$. However, influenced by the $V^{(m \neq 0)}$ matrices, in the complementary interval $\alpha_s < \alpha < \pi - \alpha_s$ (region *b*), ten trigonal distortions become the absolute minima with energy gain $E_{\text{clas}} = -g^2 \sin^2 \alpha \hbar \omega / 18$. At the boundary angles

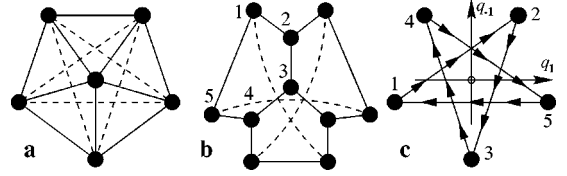


FIG. 1. The connectivity of the BO potential minima for regions *a* and *b* of angle α introduced in the text. All lines (solid and dashed) join nearest-neighbor minima. The points 1–5 of panel *b* are projected onto the q_{-1} – q_1 plane in panel *c*.

($\alpha = \alpha_s$ and $\pi - \alpha_s$), all pentagonal and trigonal minima become degenerate, and part of a continuous degenerate four-dimensional (4D) trough⁸ of depth $E_{\text{clas}} = -g^2 \hbar \omega / 28$.

We come now to the role of the Berry phase in this system. As well known, geometrical phases are induced by conical degeneracies of two BO potential surfaces.^{6,10} In the $D \otimes d$ system^{8,15} (the $\alpha = \pi - \alpha_s$ case of the model studied here) the flat minimum trough touches tangentially the second BO sheet. For that case, it was shown^{15,18} that the tangential contacts lead to null Berry phase, in turn yielding a nondegenerate ground state. For generic α in contrast, all contacts between the lowest two potential sheets occur instead as conic intersections, at points that are far from the potential minima. In particular, conical crossings appear at both trigonal and pentagonal axes for α in regions *a* and *b*, respectively (i.e., when they do not correspond to minima). For example, for \vec{q} on the \hat{q}_0 axis, Eq. (7) lists the five electronic eigenvalues, and it can be readily verified that for α in region *b* the most negative one is indeed twofold degenerate.

In region *a*, the six minima are all equidistant, defining the simplest regular polytope in 5 dimensions [see Fig. 1(a)]. In this case, therefore, minimal closed paths join any of the 20 triplets of minima. It is straightforward to verify that at the center of all such triplets there lies one of the trigonal axes, carrying a conical intersection. If the degeneracy were restricted to the trigonal axes, however, the rich topology of the 5D space would allow the triangular loop to squeeze continuously to a point avoiding the degenerate line: the associated Berry phase would then vanish. Instead, we checked that the two lowest sheets remain in contact through a bulky 3D (one radial + two tangential) region of distortions surrounding each trigonal axis. This guarantees the nontrivial topology of the loops, thus the possibility of nonzero Berry phase. Indeed a *geometrical phase of π* is associated to these triangular loops, as we compute explicitly by the discretized phase integral of Ref. 19. We expect therefore, that, for α in region *a*, the GS of the $H \otimes h$ model must show the signature of a Berry-phase entanglement.

In region *b*, the minima are ten, each with three nearest neighbors and six second neighbors. The shortest closed paths through minima joins three points such as $(1 \rightarrow 2 \rightarrow 3 \rightarrow 1)$ in Fig. 1(b). Somewhat longer paths are of pentagonal shape, such as $(1 \rightarrow 2 \rightarrow 3 \rightarrow 4 \rightarrow 5 \rightarrow 1)$. We compute the Berry phases for both kinds of paths, obtaining π and 0 for the 3-points and 5-points loop, respectively. The nontrivial phases originate at the central degeneracy, since they remain the same if the five points are squeezed around the central pentagonal axis. Indeed, the coupling matrix restricted to the lowest levels getting degenerate at the q_0 direction is

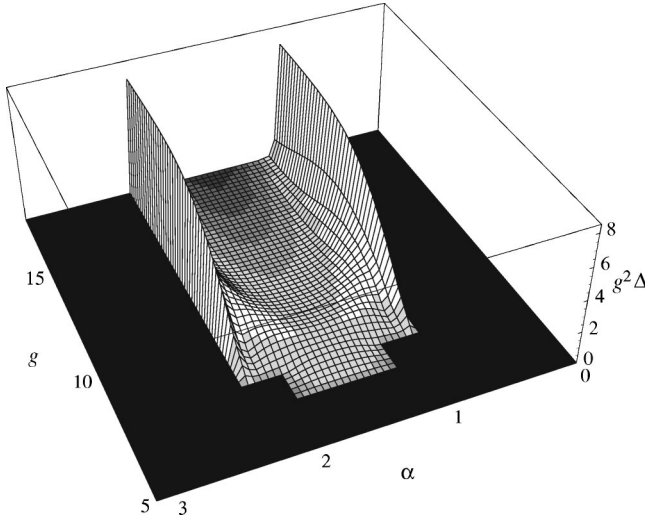


FIG. 2. g^2 times the gap $\Delta = E_H - E_A$ (units of $\hbar\omega$, logarithmic gray scale) between the lowest H and A vibronic states as a function of g and α . In the positive region, the GS is A , elsewhere it is H , and there we plot 0 for better readability. This generates on the g - α plane a zero-temperature “phase diagram.” The basis is truncated to include up to 40 oscillator states.

$$\left(\sqrt{\frac{27}{80}} \cos \alpha + \frac{\sqrt{3}}{4} \sin \alpha \right) \begin{pmatrix} -q_1 & -q_{-1} \\ -q_{-1} & q_1 \end{pmatrix}. \quad (8)$$

The distortion coordinates determining the electronic wave function are therefore q_{-1} and q_1 , and the coupling has the form of the linear $E \otimes e$ DJT, or, equivalently, of the Zeeman coupling of a spin- $\frac{1}{2}$,¹⁰ associated to a standard conical “diabolo” intersection. The pentagonal path ($1 \rightarrow 2 \rightarrow 3 \rightarrow 4 \rightarrow 5 \rightarrow 1$) in the five-dimensional q -space projects onto the $q_{-1} - q_1$ plane into the “star” drawn in Fig. 1(c). It is apparent that the pentagonal circuit loops twice around the degeneracy, while the triangular “shortcut” ($1 \rightarrow 2 \rightarrow 3 \rightarrow 1$) completes only one turn: this accounts for the computed phases.

The potential barrier separating two far neighbors ($3 \rightarrow 1$) is longer and energetically at least 60% more expensive than that linking next neighbors ($1 \rightarrow 2$). As a consequence, the overlap integral for far neighbors is approximately the square of that for next neighbors (see Ref. 9 for a special case), thus negligibly small for large g . In this limit, therefore, *only the pentagonal loops* are relevant, and so are the associated Berry phases. We conclude that, in region b , although non-trivial Berry phases are present, they have *no effect* on the strong-coupling low-energy spectrum. Thus, in particular, the GS, which, in region a of angle α , should remain H for any coupling, in region b should become a nondegenerate A state turning lower at large g . We stress that we have established the presence of nonzero Berry phases for all values of α , but also that, in region b , the geometrical phase of a certain class of loops is ineffective due to high tunneling barriers traversed by these paths.

This scenario is confirmed by numerical diagonalization (Lanczos method).^{8,20} Figure 2 displays the gap between the lowest H and A vibronic states. At weak coupling, as suggested by continuity, the GS is H . For $g > 7$ and α in range b , the A state becomes the GS. We note however a little modulation in the boundaries of this region, both g - and α -wise.

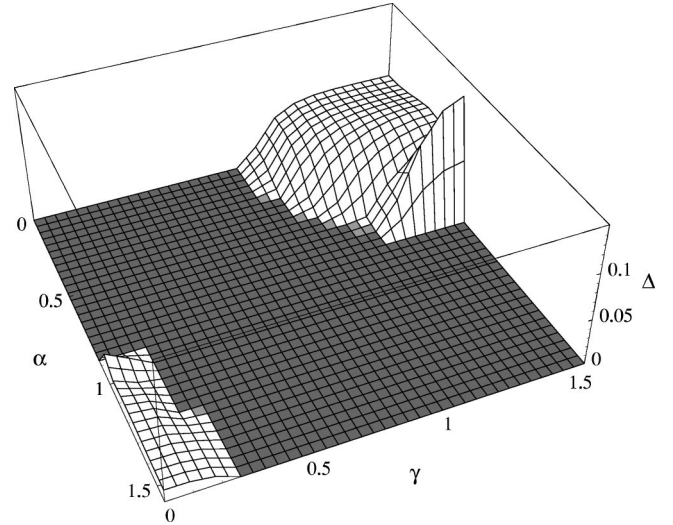


FIG. 3. The gap $\Delta = E_H - E_A$ (units of $\hbar\omega_1$) between the lowest H and A vibronic states as a function of α and γ (defined in the text), for $g=10$, $\omega_2/\omega_1=5$. In the region of $\Delta \leq 0$ (H GS), we replace the gap by 0. The convergence is fair, the basis including up to 12 oscillator states.

We observe, in particular, that the two special values α_s and $\pi - \alpha_s$, far from marking the closing of the H - A gap, show instead a rather sharp peak in the α direction. By drawing (in Fig. 2) the gap multiplied by g^2 , we evidence, along these ridges at α_s and $\pi - \alpha_s$, the g^{-2} large- g behavior of the H - A gap, characteristic of the motion in a flat trough of size $\sim g$. Inside region b , instead, the gap vanishes much more quickly due to the tunneling integral through the barriers between trigonal minima vanishing exponentially in g^2 .

It is straightforward to extend the one-mode Hamiltonian (4) to a more realistic case of many distortion modes,²¹ each characterized by its own frequency, coupling, and angle of mixing:

$$H = \sum_i [H_{\text{harm}}(\hbar\omega_i) + H_{e-v}(g_i \hbar\omega_i, \alpha_i)]. \quad (9)$$

We study in detail the two-mode case. Five free parameters (ω_1 being taken as a global scale factor) appear in the model. In order to carry out a significant study of the phase diagram, we limit ourselves to (i) two values only (1 and 5) of the ratio ω_2/ω_1 ,²² and (ii) $\alpha_2 - \pi/2 = \alpha_1 \equiv \alpha$, assuming a principle of “maximum difference” between the modes. We take advantage of spectral invariance for individual sign change of each of the couplings $g_i \rightarrow -g_i$ and for $\alpha \rightarrow -\alpha$, restricting to the $0 \leq \alpha \leq \pi/2$, $g_i > 0$ sector. For convenience, we introduce polar variables $g_1 = g \cos \gamma$, $g_2 = g \sin \gamma$ ($0 < \gamma < \pi/2$), and draw slices of the parameters space for fixed values of g , as α - γ planes.

The first interesting observation concerns the case of equal frequencies: even though Hamiltonian (9) is linear in the coupling parameters the CG coefficients and the boson operators, the special case $\omega_1 = \omega_2$ *cannot be trivially reduced to a one-mode problem*, by means of a suitable rotation mixing mode 1 and 2. This is a consequence of the linear independence of the coupling matrices $V^{(m)}(\alpha)$ for different values of α .

We resort to exact diagonalization to treat the two-mode case. Due to the larger size of the matrices, we are limited to smaller couplings: we obtain a satisfactorily converged $E_H - E_A$ gap up to $g \leq 10$ only. The calculations, for both $\omega_2/\omega_1 = 1$ and 5, show that for $g \leq 7$ the GS symmetry remains H for any α and γ as in the one-mode case. Then, already at $g = 8$, an A (nondegenerate) GS makes its appearance in two localized regions of the α - γ plane. Starting from $g \geq 9$, these separated regions assume essentially their asymptotic strong-coupling shape (see Fig. 3). The first region, located symmetrically across $\alpha = \pi/2$, corresponds mainly to mode 1 with b type (no-Berry) coupling: mode 2 (Berry-phase entangled in this region) acts as a weak perturbation, incapable to change the GS symmetry for small enough γ . On the other side, the second region of A -GS is located around $\alpha = 0$: there, it is mode 2 that is responsible for the no-Berry-phase coupling, mode 1 acting as a weak perturbation, for γ close enough to $\pi/2$. For $\omega_2/\omega_1 = 1$ (not reported here), the two A GS regions are, of course, equivalent. For $\omega_2/\omega_1 = 5$ (Fig. 3) instead, these two regions differ in size, in relation with the different relative energetics of mode 1 versus mode 2.

In conclusion, we have illustrated the importance of the tunneling energetics of paths surrounding the points of degeneracies of the two lowest BO potential sheets, for defin-

ing the effective role of the Berry phase. In all classical linear JT models, the low-energy paths are affected by the geometrical phase in a way leading to a ‘‘boring’’ fixed ground-state symmetry. The $H \otimes h$ model is special in being determined by an additional parameter, that changes the connectivity of the graph of low-energy paths through minima, along with the regions of degeneracy of the two lowest sheets. Consequently, this parameter leads continuously from a regular, Berry-phase entangled region to a whole region where, although present, the Berry phase is totally ineffective in imposing its selection rules to the low-energy vibronic states, and to the GS in particular.

In particular, in the molecular ion C_{60}^+ , the H electronic state couples to eight h modes (and also to six g modes). The present work implies that such a basic property as the symmetry of the molecular GS is not obviously known *a priori*: it depends on the detailed values not only of the coupling parameters g_i , but also of the characteristic angles α_i of each mode. We suggest that, in the lack of microscopic calculations, spectroscopical investigation should resolve this issue experimentally.

We thank Arnout Ceulemans, Brian Judd, Fabrizia Negri, Erio Tosatti, and Lu Yu for useful discussions.

-
- ¹R. Englman, *The Jahn Teller Effect in Molecules and Crystals* (Wiley, London, 1972).
- ²I. B. Bersuker and V. Z. Polinger, *Vibronic Interactions in Molecules and Crystals* (Springer-Verlag, Berlin, 1989).
- ³E. Lo and B. R. Judd, Phys. Rev. Lett. **82**, 3224 (1999).
- ⁴J. Ihm, Phys. Rev. B **49**, 10 726 (1994).
- ⁵A. Auerbach, N. Manini, and E. Tosatti, Phys. Rev. B **49**, 12 998 (1994).
- ⁶C. A. Mead, Rev. Mod. Phys. **64**, 51 (1992).
- ⁷*Geometric Phases in Physics*, edited by A. Shapere and F. Wilczek (World Scientific, Singapore, 1989).
- ⁸P. De Los Rios, N. Manini, and E. Tosatti, Phys. Rev. B **54**, 7157 (1996).
- ⁹C. P. Moate, M. C. M. O’Brien, J. L. Dunn, C. A. Bates, Y. M. Liu, and V. Z. Polinger, Phys. Rev. Lett. **77**, 4362 (1996).
- ¹⁰M. V. Berry, Proc. R. Soc. London, Ser. A **392**, 45 (1984).
- ¹¹F. S. Ham, Phys. Rev. Lett. **58**, 725 (1987).
- ¹²S. E. Apsel, C. C. Chancey, and M. C. M. O’Brien, Phys. Rev. B **45**, 5251 (1992).
- ¹³M. C. M. O’Brien, Phys. Rev. B **53**, 3775 (1996).
- ¹⁴A. Ceulemans and P. W. Fowler, J. Chem. Phys. **93**, 1221 (1990).
- ¹⁵N. Manini and P. De Los Rios, J. Phys.: Condens. Matter **38**, 8485 (1998).
- ¹⁶P. H. Butler, *Point Group Symmetry Applications* (Plenum, New York, 1981).
- ¹⁷We shall stick here to Butler’s convention (Ref. 16), and choose the m_i indexes, labeling states within the degenerate representations by the algebraic chain of subgroups $I \supset D5 \supset C5$.
- ¹⁸P. De Los Rios and N. Manini, in *Recent Advances in the Chemistry and Physics of Fullerenes and Related Materials*, edited by K. M. Kadish and R. S. Ruoff (The Electrochemical Society, Pennington, NJ, 1997), Vol. 5, p. 468.
- ¹⁹R. Resta, Rev. Mod. Phys. **66**, 899 (1994).
- ²⁰N. Manini and E. Tosatti, in *Recent Advances in the Chemistry and Physics of Fullerenes and Related Materials*, edited by K. M. Kadish and R. S. Ruoff (The Electrochemical Society, Pennington, NJ, 1995), Vol. 2, p. 1017.
- ²¹N. Manini and E. Tosatti, Phys. Rev. B **58**, 782 (1998).
- ²²The diagram for $\omega_2/\omega_1 = 5$ yields also the ground-state symmetry for the case $\omega_2/\omega_1 = 1/5$, with g_1 and g_2 exchanged (i.e., $\gamma \rightarrow \pi/2 - \gamma$ and $\alpha \rightarrow \alpha + \pi/2$).